Investigating Nonlinear Femtosecond Pulse Propagation with Frequency-Resolved Optical Gating

Hilary K. Eaton, Tracy S. Clement, *Member, IEEE,* Alex A. Zozulya, and Scott A. Diddams

(Invited Paper)

***Abstract*— Frequency-resolved optical gating (FROG) is used to investigate nonlinear pulse propagation in normally dispersive media. We present high-dynamic-range measurements of broad-bandwidth femtosecond pulses that result from nonlinear propagation in fused silica and compare these measurements with a $(3+1)$-dimensional modified nonlinear Schrödinger equation. We also demonstrate the ability of FROG to provide information about a noninstantaneous nonlinearity in methanol. In this case, the instantaneous nonlinear index and the time response of the noninstantaneous nonlinearity are used as fit parameters in a $(1+1)$-dimensional model.**

***Index Terms*—Nonlinear optics, optical propagation in nonlinear media, optical pulse measurements, ultrafast optics.**

I. Introduction

A CLEAR picture of the propagation of femtosecond laser pulses is of fundamental importance to many scientific and technological applications. A few examples include propagation in waveguides [1], [2], femtosecond lasers [3]–[6], biological systems, and the atmosphere [7]–[10]. Although some applications rely primarily on the delta-function qualities of a femtosecond pulse (e.g., time-resolved gating, transmission of binary data), at a more fundamental level pulse propagation encompasses much more than the simple transport of energy. It is a basic fact of the Maxwell equations that the manner in which a field propagates is fundamentally tied (via the polarization) to the properties of the medium in which it travels. From the standpoint of femtosecond diagnostics, this implies that if one can accurately characterize the electric field after propagation through a medium of interest, then valuable information about the medium and the propagation process may be obtained. Indeed, the underlying goal of this paper is to demonstrate that this can be accomplished with the use of frequency-resolved optical gating (FROG).

Many femtosecond propagation issues are related to the broad bandwidth of the field and the linear dispersion of the material/system through which the pulse travels. This problem has been dealt with in detail, and the careful management of linear dispersion has led to the generation and amplification of the shortest optical pulses [11]–[14]. More typical, however, is the situation in which both linear and nonlinear effects are present. Within the framework of the nonlinear Schrödinger equation, this has been a topic of study for many years [15]–[17]. Nonetheless, propagation details of femtosecond pulses at the highest powers have remained elusive. As peak powers increase to several times the critical power for self-focusing, combined linear and nonlinear effects result in complicated spatio-temporal reshaping of the pulse. The propagation dynamics are no longer described by the standard nonlinear Schrödinger equation and higher order effects must be considered [18]–[26]. At the highest powers, yet before material breakdown occurs, one observes extreme broadening of the pulse spectrum—or continuum generation [27]–[31]. As this high-power regime becomes more widely used in frequency conversion [32], spectral broadening [13], [33], [34], and parametric amplification [35], [36], a complete understanding of the propagation dynamics becomes critical.

In the past, femtosecond nonlinear pulse propagation has been studied by spectral observations [37], [38], autocorrelations [17], and cross correlations [27]. Information about the spatial effects of nonlinear propagation have been obtained using the z-scan technique [39], [40]. Although these techniques provide important information about ultrafast nonlinear propagation, they generally require assumptions about the field, and they do not provide information about the temporal phase of the electric field. In recent years, several advanced techniques have been developed that provide "full-field" information about both the amplitude and phase of the complex electric field envelope [41]–[48]. Among these, the FROG technique has emerged as a powerful, robust, and widely used diagnostic in ultrafast science [49]. It presents a researcher with the unique opportunity of directly "seeing" both the amplitude and the phase of the pulse and enables more quantitative comparisons with theoretical analysis. Although FROG has

Manuscript received September 17, 1998.

H. K. Eaton is with JILA, the University of Colorado, Boulder, CO 80309-0440 USA.

T. S. Clement was with JILA, the University of Colorado, Boulder, CO 80309-0440 USA. She is now with the National Institute of Standards and Technology, Boulder, CO 80309-0440 USA.

A. A. Zozulya is with the Department of Physics, Worcester Polytechnic Institute, Worcester, MA 01609-2280 USA.

S. A. Diddams is with JILA, the University of Colorado, Boulder, CO 80309-0440 USA, and also with the National Institute of Standards and Technology, Boulder, CO 80309-0440 USA.

Publisher Item Identifier S 0018-9197(99)02552-X.

primarily functioned as a diagnostic of laser systems [50]–[52], it also holds value as a tool for measuring nonlinear material properties [53] and studying propagation in fibers and gases [54]–[57].

In this paper, we present results that illustrate our use of FROG as an advanced diagnostic tool for the study of nonlinear pulse propagation in bulk media. We summarize how FROG measurements have enabled us to unravel and understand key features of the $(3+1)$-dimensional spatio-temporal dynamics of femtosecond laser pulses in nonlinear media with normal dispersion [25], [58], [59]. Crucial to this study is the high-dynamic-range measurement (and recovery) of FROG spectrograms with total bandwidths greater than 100 nm, which we describe in Sections II and III. In addition, in Section IV, we demonstrate how the "full-field" measurement capabilities of FROG enable one to measure time-dependent nonlinearities having a response time much less than the pulse duration.

II. Experimental Details

A regeneratively amplified Ti:sapphire laser system, operating at 1 kHz, provides the laser pulses used in all of the following experiments. The energy per pulse at the output of the system is 850 μJ. The pulses have a temporal duration of $\sim$80 fs measured at the full width at half maximum (FWHM) of intensity and are spectrally centered at 800 nm. The near bandwidth-limited pulses have a spectral FWHM of 12 nm.

For these propagation experiments, it is necessary to use a measurement technique capable of resolving both the high- and low-intensity regions of the pulse. Propagation of intense femtosecond pulses through several centimeters of a bulk nonlinear medium such as fused silica can result in complicated temporal and spectral intensity profiles, as well as dramatic spectral broadening. As an example, the intensity in the wings of the spectrum after propagation (at wavelengths that are $\geq$50 nm from the spectral peak) can be just three orders of magnitude less than the peak intensity. Compare this to our input pulse, where the intensity spans six orders of magnitude over the same 50-nm spectral region. To record the information in the spectral wings, it is necessary to have a high-dynamic-range broad-bandwidth measurement technique such as the second-harmonic generation (SHG) form of FROG. The $\chi^{(2)}$-based SHG FROG, when used in a multishot configuration, can be more than 1000 times more sensitive than variations of FROG based on third-order nonlinearities [49].

Details of FROG apparatus and retrieval algorithms have been described in detail elsewhere [49], and a discussion of SHG FROG and the experimental issues associated with measurement of broad-band 10-fs pulses can be found in a publication by Taft *et al.* [51]. Here, we discuss specific design parameters relevant to making high-dynamic-range measurements of complicated broad-band pulses. A diagram of the SHG FROG apparatus is shown in Fig. 1. The pulse to be measured is split into two replicas using a 1.6-mm-thick beamsplitter with a broad-band Inconel coating. Front surface metallic reflectors are used to minimize dispersion as the pulse propagates to the frequency-conversion crystal. A 10-cm focal length spherical mirror focuses the two replicas of the pulse into the second-harmonic conversion crystal, and the resulting signal at 2ω is imaged onto the entrance slits of an imaging spectrometer. The pulse in one arm of the interferometer is delayed with respect to the other by a stepper-motor controlled translation stage. The spectrum at each delay is recorded with a thermoelectrically cooled 16-bit CCD camera. Typical peak intensities recorded on the camera produce 50 000 counts, while the dark current level is at 970 counts. In addition, the noise level is $\sim$2–5 counts, providing a signal-to-noise ratio (SNR) of better than 10 000:1.

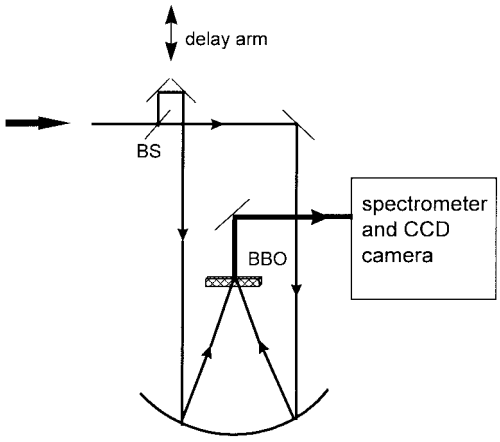

Fig. 1. Schematic of SHG FROG apparatus. The beam splitter is denoted BS. The second-harmonic crystal is a 50-μ-thick piece of BBO. All other optics are metal mirrors.

Because of the large spectral bandwidths of the propagated fields, it is important to take into account the finite phase-matching bandwidth of the second-harmonic conversion process. This finite phase-matching bandwidth arises from a phase mismatch between the fundamental and second-harmonic frequencies. The conversion efficiency due to phase mismatch is given by [60], [61]

$$\eta = \left[\frac{\sin(\Delta k L/2)}{\Delta k L/2}\right]^2 \tag{1}$$

where $\Delta k = (2\omega/c)[n_e(2\omega,\theta) - n_o(\omega)]$, ω and 2ω are the fundamental and second-harmonic frequencies, n_e and n_o are the extraordinary and ordinary refractive indices, L is the length of the crystal, and θ is the phase-matching angle in the crystal. Therefore, the thinner the crystal, the larger the range of frequencies that can be converted for a given crystal orientation. We use a 50-μm-thick piece of β-BaB_2O_4 (BBO), cut at an angle of $\theta = 29.1^\circ$ for type-I phase matching at 800 nm. The phase-matching efficiency for the crystal used in these experiments has a FWHM of 60 nm. The pulses measured in these experiments typically have a bandwidth after conversion to the second harmonic of $\sim$40 nm (FWHM), thus the phase-matching bandwidth provided by this crystal is sufficient for conversion of most of the spectrum. The fact that the conversion efficiency is not constant over the entire bandwidth of the pulse does not present a formidable problem because this can be corrected by using the consistency checks provided by FROG marginals. As has been demonstrated previously [51], the FROG trace is corrected prior to being

input into the retrieval algorithm by using the frequency marginal and the autoconvolution of the pulse spectrum. This correction eliminates bandwidth limitations due to finite phase-matching efficiencies, as well as grating and detector responses. Comparison of the frequency marginal with the autoconvolution of the fundamental spectrum is also used for alignment of the second-harmonic conversion crystal. The angle of the crystal is tuned for the smallest difference between the autoconvolution and the frequency marginal. At this angle, there is optimal overlap of the conversion efficiency curve with the second-harmonic pulse spectrum.

III. Broad-Bandwidth Measurements

In this section, we present data that demonstrate the ability of SHG FROG to recover broad-band temporally complex pulses, and we illustrate how these measurements impact development of propagation theories. In the experiments, the amplified pulses are strongly attenuated, spatially filtered, and focused with a $f = +50$ cm lens to a waist at the input face of a 30-mm-long fused silica sample. The spot size at the entrance face of the sample is 70 μm FWHM, and the peak power is 5.0 MW. After passing through the sample, the light diffracts freely over 1.5 m to the FROG apparatus where the on-axis portion of the beam is selected with a $\sim$1-mm aperture. FROG spectrograms are recorded on a 256×256 grid, with a time step of 8 fs and a wavelength step of 0.297 nm. For each value of the delay, the signal is averaged over 300 pulses.

Gray scale intensity plots of the measured and retrieved FROG trace under these conditions are shown in Fig. 2. The square root of the second-harmonic intensity is shown for display purposes to emphasize the wings of each trace. Darker shading corresponds to higher intensity regions, and a contour plot with a contour interval of 40 units is overlaid on each trace. The actual intensity values (not the square root) range from 2 to $\sim$45 000 counts. Very good agreement between the two traces is seen, even at the lowest intensity values. As discussed previously, the thin second-harmonic crystal used in these experiments enables the full second-harmonic spectrum of the pulse to be measured.

Fig. 3 shows the spectrum recovered from the FROG algorithm (dashes) and an independently measured fundamental spectrum (solid line) corresponding to the data in Fig. 2. The spectra are plotted on a log scale to emphasize the very good agreement in the wings, down to the noise level of the spectrometer. The short wavelength side of the measured fundamental spectrum cuts off before the noise level is reached due to the spectrum extending beyond the edge of the CCD camera in the spectrometer. The excellent agreement between the two spectra demonstrates the high-dynamic-range capabilities of SHG FROG which make it suitable for characterizing the broad-bandwidth pulses that can result from nonlinear propagation.

The temporal intensity and phase of the propagated pulse retrieved from the FROG data of Fig. 2 are shown in Fig. 4(a). After propagation, the 80-fs input pulse has split into two pulses of shorter time duration. The overall phase curvature is indicative of an up-chirp across the split pulses such that

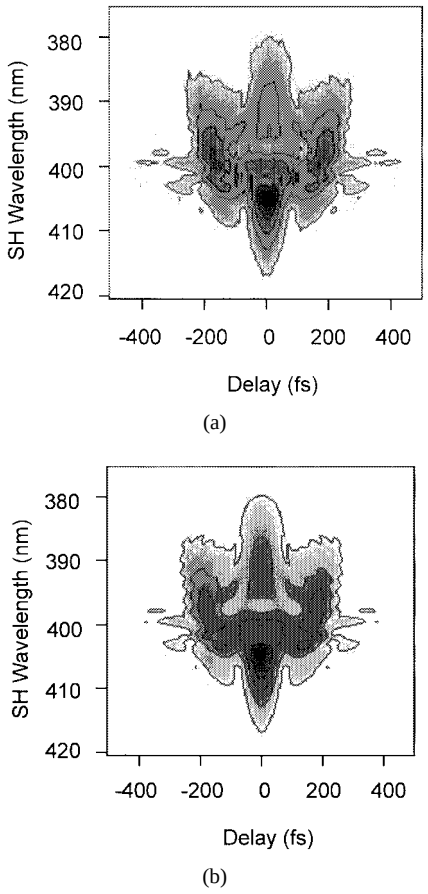

Fig. 2. (a) Measured and (b) recovered FROG traces of a temporally split pulse. The square root of the intensity (gray scale) of the traces is plotted in order to emphasize the low-intensity wings (lighter shading). A contour plot with a contour interval of 40 units is overlaid on each plot.

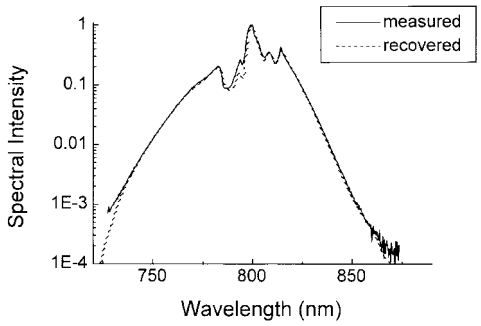

Fig. 3. Pulse spectrum (dashes) corresponding to the recovered FROG trace shown in Fig. 2 and an independently measured spectrum (solid line). Note that the spectral intensity is plotted on a log scale.

the leading pulse is red-shifted spectrally with respect to the trailing pulse. The time ambiguity inherent in SHG FROG can be removed in three ways: 1) repeat the measurement after chirping the pulse in a known manner, such as propagating the pulse through a glass with known dispersion; 2) propagate through a thin piece of glass such that surface reflections introduce a small pulse behind the main pulse [51]; or 3) have some *a priori* understanding of the processes that produced the measured pulse. We choose the third option, using information from our developing model of pulse propagation as described in greater detail below [25], [59]. We note that we have also

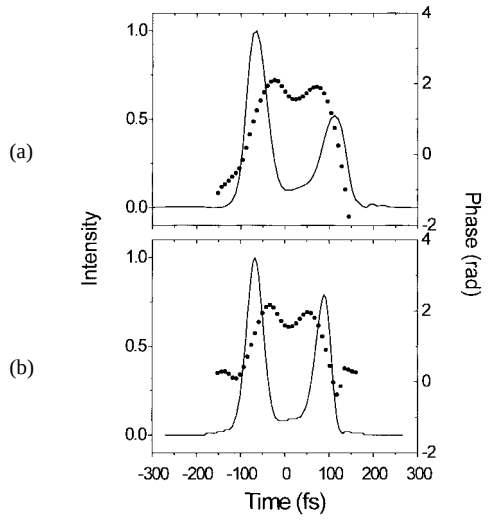

Fig. 4. (a) Measured and (b) calculated temporal fields. Intensity is plotted along the left axis and is shown as a solid line. Phase is shown as points and is plotted along the right axis. The calculated field assumes a flat-phase Gaussian pulse as input. The experimental input peak power for (a) is 5.0 MW.

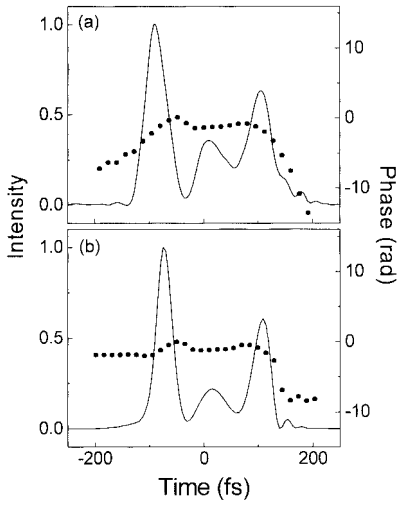

Fig. 5. (a) Measured and (b) calculated temporal fields demonstrating multiple splitting. Intensity is plotted along the left axis and is shown as a solid line. Phase is shown as points and is plotted along the right axis. The experimental input peak power for (a) is 5.6 MW.

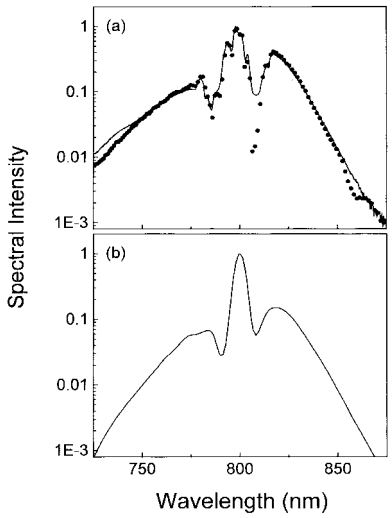

Fig. 6. (a) Measured and (b) calculated spectra corresponding to the data of Fig. 5. In (a), the solid line is the spectrum measured directly with a 0.27-m spectrometer and a CCD, while the points are the Fourier transform of the SHG-FROG measurement of Fig. 5(a).

checked our assumptions with propagation through a 5-cm-thick piece of BK-7.

Initial attempts to model propagation in this regime relied on a simple $(3+1)$-dimensional nonlinear Schrödinger equation [15]–[17]. Although this simple model did predict pulse splitting, experimental data showed asymmetries in the split pulses that the model could not reproduce [58]. Observation of this asymmetry led to the inclusion of additional effects in the model, such as a Raman nonlinearity, space–time focusing, and nonlinear shock [18], [20], [24], [25], [59]. As the model evolved, numerical results provided direction about which experimental parameters could be varied to better test the model itself. In this way, the model and our understanding of nonlinear pulse propagation have been iteratively improved. The current $(3+1)$-dimensional model takes into account the Raman effect, space–time focusing, nonlinear shock terms, and third-order dispersion [25]. In addition, we have found it necessary to include in the theoretical analysis the diffraction of the field from the output face of the fused silica (near field) to the FROG apparatus (far field) [62]. The field predicted by this model is shown in Fig. 4(b). The initial condition of the model is a real Gaussian in space and time, with spatial and temporal FWHM equal to the measured values of the input pulse. All other parameters are those of fused silica. As seen, the numerical simulation correctly predicts the asymmetric pulse splitting, and the measured and calculated phase are also in very good agreement. The small differences between the measured and calculated fields are most likely a result of the experimental input pulse possessing spatial and temporal aberrations that make it differ from the ideal transform-limited Gaussian.

One interesting question that has previously remained unanswered in this regime is whether the two pulses seen in Fig. 4 undergo a secondary splitting as the input power is increased. Our SHG FROG measurements have provided a definitive answer to this question. As shown in Fig. 5, multiple splittings do arise when the input power to the fused silica sample is increased to 5.6 MW. Here we present both the measured and calculated temporal intensity and phase of the field. The corresponding measured and calculated spectra are shown in Fig. 6. All major features, in both the time and frequency domains, are reproduced by the theory.

We note that clear multiple splitting, as seen in Fig. 5(a), only occurs in the far field. More generally, we have found that the position of maximum self-focusing (which occurs in the medium) and the position of pulse splitting are spatially separated. The pulse first self-focuses, and then at some later propagation distance it splits, with the distance between the self-focusing event and the splitting being inversely proportional to the input power. We have also made measurements at even higher input powers—in the regime where the bright continuum generation extends below 400 nm. In this situation,

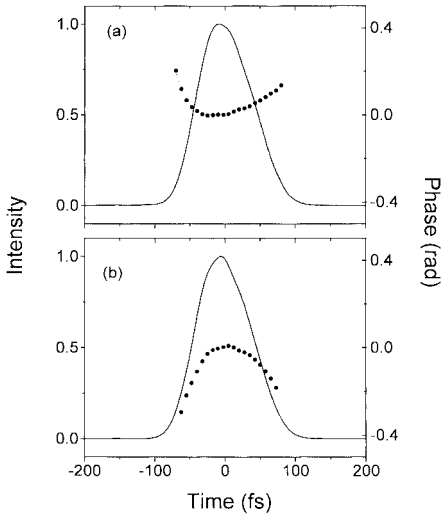

Fig. 7. Intensity (solid lines) and phase (points) of a pulse both (a) prior to and (b) after propagation through a 1-cm sample of methanol.

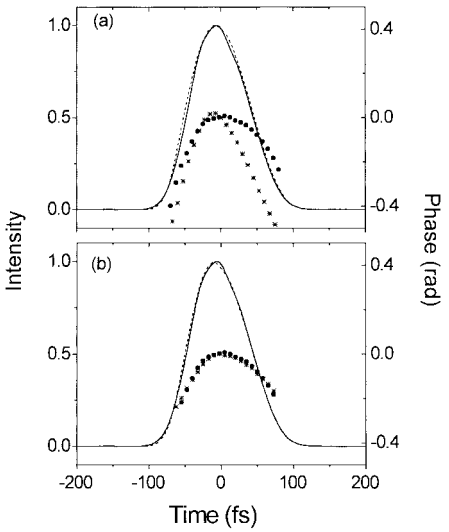

Fig. 8. Calculated field after propagation assuming (a) an instantaneous nonlinearity and (b) with inclusion of a noninstantaneous nonlinearity. Calculated intensity is plotted as a dashed line. The calculated phase is shown as asterisks. The calculated fields are shown along with the measured field (solid line and points) for comparison.

we find that the the field loses the sharper details seen in Fig. 5, and the multiple peaks coalesce toward a single broad pulse. Further details of these spatio-temporal dynamics are reported elsewhere [62].

IV. Time-Dependent Nonlinearities

In addition to nonlinear propagation dominated by instantaneously responding nonlinearities, FROG can be used to study propagation when significant contributions from noninstantaneous nonlinearities are present as well. Because FROG provides a measure of the phase as well as the intensity of the pulse, it is possible to directly observe the change in phase that occurs as as result of the noninstantaneous nonlinear response. Instantaneous nonlinearities are characterized by a phase shift that directly follows the intensity of the pulse. Noninstantaneous nonlinearities can be expressed as a convolution of the instantaneous nonlinear response with a time-dependent onset function, resulting in a shift of the peak of the phase toward the trailing edge of the pulse. In this section, we detail measurements of a noninstantaneous nonlinear response in methanol.

In these experiments, the unfocused beam propagates approximately as a plane wave in the sample, with a diameter of 5 mm (FWHM). The energy per pulse of 227 μJ corresponds to a peak power of 2.6 GW. Because of the high energy of the pulses, the beam is not spatially filtered. The beam propagates through a 1-cm path length of methanol that is contained in a spectrophotometer cell. Propagation through only the two 1-mm-thick cell walls was found to have negligible effect on the pulses at this intensity.

Fig. 7 shows the measured intensity and phase of a pulse prior to and after propagation through the methanol sample. The input field is shown in (a) and the field after propagation through the methanol sample is shown in (b). In both graphs, the solid line represents the intensity and the dots represent the phase. The upward curvature of the phase in (a) is evidence of an initially down-chirped input. After propagation through the methanol, the pulse is noticeably up-chirped as a result of the positive group velocity dispersion and the positive nonlinear index of refraction n_2. In addition, the peak of the phase curvature has been shifted slightly toward the trailing edge of the pulse.

Since we have chosen conditions such that the pulse propagates through the sample as a plane wave, we can model the propagation using a simple $(1+1)$-dimensional nonlinear Schrödinger equation

$$\frac{\partial \mathcal{E}}{\partial z} + i\frac{k''}{2}\frac{\partial^2 \mathcal{E}}{\partial t^2} - i\frac{2\pi n_2}{\lambda}|\mathcal{E}|^2\mathcal{E} = 0. \tag{2}$$

The second term of this equation accounts for group velocity dispersion, and the third term gives the instantaneous nonlinearity. The measured input field shown in Fig. 7(a) is used as input to this model, with $k'' = 290$ fs^2/cm [63] and $n_2 = 8 \times 10^{-16}$ cm^2/W. The calculated field after propagation is shown in Fig. 8(a) along with the measured field for comparison. The calculated intensity and phase are given by the dashed line and the asterisks respectively. The simulation was performed using a range of different n_2 values around those found in the literature [64], [65], and no significant difference in the fit was observed. As illustrated by this example, the simple model, including reasonable values for the material parameters and an instantaneous response time for the nonlinearity, fails to match the experimentally measured phase, especially the shift in the phase to later times.

This shortcoming in the model can be corrected by phenomenologically including a noninstantaneous response of the nonlinearity such that the term

$$n_2|\mathcal{E}|^2 \tag{3}$$

in (2) is replaced by [15]

$$\int_{-\infty}^{t} \frac{n_2|\mathcal{E}(t')|^2}{2\tau}\exp\left(-\frac{t-t'}{\tau}\right)dt' \tag{4}$$

where τ is the exponential response time of the nonlinearity.

Fig. 8(b) shows the results of the model including the delayed response term of (4) with $\tau = 10$ fs. The measured input field of Fig. 7(a) was again used as input to the model. The calculated intensity is plotted as a dashed line, and the phase is shown as asterisks. Inclusion of the noninstantaneous response correctly predicts the observed shifting of the peak of the phase toward the trailing edge of the pulse. The calculated phase best matches the experimentally determined phase when values of $n_2 = 8 \times 10^{-16}$ cm^2/W and $\tau = 10$–20 fs are used in the model. Previous experiments by Nibbering *et al.* [64] determined a value of $\tau = 27$ fs for the nonlinear response time in methanol. Future experiments are planned that will utilize a high-power vacuum spatial filter in the laser beam path and a flowing cell for the methanol in order to provide a more stable beam for the SHG-FROG measurements and reduce the uncertainty in the value of the response time.

An interesting feature of the data in Fig. 8 is the extremely small value of the exponential response time τ. Response times for electrostriction and thermal effects are on the order of nanoseconds, molecular reorientation occurs on the order of 10^{-11} s, and molecular librations respond on a timescale of about 100 fs [29], but all of these are too slow to explain our observations. It may be possible that a rotational Raman excitation is responsible for the time-delayed nonlinearity we observe. Another possibility is that the delay arises from the presence of a nearby two-photon absorption resonance.

Propagation in fused silica in this plane-wave regime shows no evidence of a noninstantaneous nonlinearity [58]. If fused silica does have a nonlinear response given by (4), the response time is so small that the shift in the phase could not be observed with the (relatively) long pulses we use here. Perhaps experiments using very short, e.g., 5 fs, pulses would be able to resolve a noninstantaneous nonlinearity in fused silica.

The data presented in this section clearly demonstrate the value of FROG for the study of propagation in systems in which both an instantaneous and a delayed response of the medium are present. The FROG technique provides a way of measuring noninstantaneous responses that are shorter than the duration of the pulse itself. In addition, shorter pulses could be used to interrogate media with extremely fast yet still noninstantaneous time delays. If one wishes to look at samples with longer delayed responses, it should be possible to do so with a longer input pulse.

V. Conclusion

This paper demonstrates that FROG is not only useful as a laser diagnostic technique, but that it can also be a powerful tool for use in experiments involving ultrashort laser pulses. We have shown also that SHG FROG is capable of high-dynamic-range measurements of complicated pulses having well over 100 nm of total spectral bandwidth. Experiments in the pulse-splitting regime exemplify the mutually beneficial relationship that is possible between experiment and theory and demonstrate the ability of FROG to lend insight into the nature of complex propagation problems. We have also demonstrated the ability of FROG to follow nonlinear propagation in systems where both instantaneous and noninstantaneous nonlinearities are present. Clearly, the "full-field" information provided by FROG offers an advantage over the more traditional methods of investigating pulse propagation and should prove valuable in understanding the physics underlying other interesting and challenging problems in a variety of fields.

References

[1] G. P. Agrawal, *Nonlinear Fiber Optics*. San Diego, CA: Academic, 1989.

[2] R. McLeod, K. Wagner, and S. Blair, "$(3+1)$-dimensional optical soliton dragging logic," *Phys. Rev. A*, vol. 52, pp. 3254–3278, 1995.

[3] F. Krausz, M. E. Fermann, T. Brabec, P. F. Curley, M. Hofer, M. H. Ober, C. Spielmann, E. Wintner, and A. J. Schmidt, "Femtosecond solid-state lasers," *IEEE J. Quantum Electron.*, vol. 31, pp. 788–790, 1995.

[4] J. Zhou, G. Taft, C.-P. Huang, M. M. Murnane, and H. C. Kapteyn, "Pulse evolution in a broad-bandwidth Ti:sapphire laser," *Opt. Lett.*, vol. 19, pp. 1149–1151, 1994.

[5] H. A. Haus, "Theory of mode locking with a slow saturable absorber," *IEEE J. Quantum Electron.*, vol. QE-11, p. 736, 1975.

[6] F. X. Kärtner, I. D. Jung, and U. Keller, "Soliton mode-locking with saturable absorbers," *IEEE J. Select. Topics Quantum Electron.*, vol. 2, pp. 540–556, 1996.

[7] X. M. Zhao, J.-C. Diels, C. Y. Wang, and J. Elizondro, "Femtosecond ultraviolet laser pulse induced lightning discharges in gases," *IEEE J. Quantum Electron.*, vol. 31, pp. 599–612, 1995.

[8] A. Braun, G. Korn, X. Liu, D. Du, J. Squier, and G. Mourou, "Self-channeling of high-peak-power femtosecond laser pulses in air," *Opt. Lett.*, vol. 20, pp. 73–75, 1995.

[9] E. T. J. Nibbering, P. F. Curley, G. Grillon, B. S. Prade, M. A. Franco, F. Salin, and A. Mysyrowicz, "Conical emission from self-guided femtosecond pulses in air," *Opt. Lett.*, vol. 21, pp. 62–64, 1996.

[10] L. Woeste, S. Wedeking, J. Wille, P. Rairouis, B. Stein, S. Nikolov, C. Werner, S. Niedermeier, F. Ronneberger, H. Schillinger, and R. Sauerbrey, "Femtosecond atmospheric lamp," *Laser und Optoelektronik*, vol. 29, pp. 51–53, 1997.

[11] R. L. Fork, C. H. Brito-Cruz, P. C. Becker, and C. V. Shank, "Compression of optical pulses to six femtoseconds by using cubic phase compensation," *Opt. Lett.*, vol. 12, pp. 483–485, 1987.

[12] C. P. J. Barty, T. Guo, C. Le Blanc, F. Raksi, C. Rose-Petruck, J. Squier, K. R. Wilson, V. V. Yakovlev, and K. Yamakawa, "Generation of 18-fs, multiterawatt pulses using regenerative pulse shaping and chirped pulse amplification," *Opt. Lett.*, vol. 21, pp. 668–670, 1996.

[13] A. Baltuska, Z. Wei, M. S. Pshenichnikov, D. A. Wiersma, and R. Szipőcs, "All-solid-state cavity-dumped sub-5-fs laser," *Appl. Phys. B*, vol. 65, pp. 175–188, 1997.

[14] S. Backus, C. G. Durfee, M. M. Murnane, and H. C. Kapteyn, "High power ultrafast lasers," *Rev. Sci. Instrum.*, vol. 69, pp. 1207–1223, 1998.

[15] J. H. Marburger, "Self-focusing: Theory," *Prog. Quantum Electron.*, vol. 4, pp. 35–110, 1975.

[16] J. E. Rothenberg, "Pulse splitting during self-focusing in normally dispersive media," *Opt. Lett.*, vol. 17, pp. 583–585, 1992.

[17] J. K. Ranka, R. W. Schirmer, and A. L. Gaeta, "Observation of pulse splitting in nonlinear dispersive media," *Phys. Rev. Lett.*, vol. 77, pp. 3783–3786, 1996.

[18] J. Rothenberg, "Space-time focusing: Breakdown of the slowly varying envelope approximation in the self-focusing of femtosecond pulses," *Opt. Lett.*, vol. 17, pp. 1340–1342, 1992.

[19] G. G. Luther, J. V. Moloney, A. C. Newell, and E. M. Wright, "Self-focusing threshold in normally dispersive media," *Opt. Lett.*, vol. 19, pp. 862–864, 1994.

[20] J. T. Manassah and B. Gross, "Self-focusing of $(3+1)$-d femtosecond pulses in nonlinear Kerr media," *Laser Physics*, vol. 6, pp. 563–578, 1996.

[21] G. Fibich and G. C. Papanicolaou, "Self-focusing in the presence of small time dispersion and nonparaxiality," *Opt. Lett.*, vol. 22, pp. 1379–1381, 1997.

[22] T. Brabec and F. Krausz, "Nonlinear optical pulse propagation in the single-cycle regime," *Phys. Rev. Lett.*, vol. 78, pp. 3282–3285, 1997.

[23] Q. Feng, J. V. Moloney, A. C. Newell, E. M. Wright, K. Cook, P. K. Kennedy, D. X. Hammer, B. A. Rockwell, and C. R. Thompson, "Theory and simulation on the threshold of water breakdown induced by focused ultrashort laser pulses," *IEEE J. Quantum Electron.*, vol. 33, pp. 127–137, 1997.

[24] J. K. Ranka and A. L. Gaeta, "Breakdown of the slowly-varying envelope approximation in the self-focusing of ultrashort pulses," *Opt. Lett.*, vol. 23, pp. 534–536, 1998.
[25] A. A. Zozulya, S. A. Diddams, and T. S. Clement, "Numerical investigations of nonlinear femtosecond pulse propagation with the inclusion of Raman, shock, and third-order phase effects," *Phys. Rev. A*, vol. 58, no. 4, pp. 3303–3310, 1999.
[26] M. Mlejnek, E. M. Wright, and J. V. Moloney, "Dynamic spatial replenishment of femtosecond pulses propagating in air," *Opt. Lett.*, vol. 23, pp. 382–384, 1998.
[27] R. L. Fork, C. V. Shank, C. Hirlimann, and R. Yen, "Femtosecond white-light continuum pulses," *Opt. Lett.*, vol. 8, pp. 1–3, 1983.
[28] P. B. Corkum and C. Rolland, "Femtosecond continua produced in gases," *IEEE J. Quantum Electron.*, vol. 25, pp. 2634–2639, 1989.
[29] R. R. Alfano, *The Supercontinuum Laser Source*. New York: Springer-Verlag, 1989.
[30] H. Nishioka, W. Odajima, K. Ueda, and H. Takuma, "Ultrabroadband flat continuum generation in multichannel propagation of terrawatt Ti:sapphire laser pulses," *Opt. Lett.*, vol. 20, pp. 2505–2507, 1995.
[31] A. Brodeur and S. L. Chin, "Band-gap dependence of ultrafast white-light continuum," *Phys. Rev. Lett.*, vol. 80, no. 20, pp. 4406–4409, 1998.
[32] C. G. Durfee III, S. Backus, M. M. Murnane, and H. C. Kapteyn, "Ultrabroadband phase-matched optical parametric generation in the ultraviolet by use of guided waves," *Opt. Lett.*, vol. 22, pp. 1565–1567, 1997.
[33] M. Nisoli, S. De Silvestri, and O. Svelto, "Generation of high energy 10 fs pulses by a new pulse compression technique," *Appl. Phys. Lett.*, vol. 68, pp. 2793–2795, 1996.
[34] E. T. J. Nibbering, G. Grillon, M. A. Franco, B. S. Prade, and A. Mysyrowicz, "Determination of the inertial contribution to the nonlinear refractive index of air, n_2, and o_2 by use of unfocused high-intensity femtosecond laser pulses," *J. Opt. Soc. Amer. B*, vol. 14, pp. 650–660, 1997.
[35] G. Cerullo, M. Nisoli, S. Stagira, and S. De Silvestri, "Sub-8-fs pulses from an ultrabroadband optical parametric amplifier in the visible," *Opt. Lett.*, vol. 23, pp. 1283–1285, 1998.
[36] A. Shirakawa, I. Sakane, and T. Kobayashi, "Pulse-front-matched optical parametric amplification for sub-10-fs pulse generation tunable in the visible and near infrared," *Opt. Lett.*, vol. 23, pp. 1292–1294, 1998.
[37] F. Reynaud, F. Salin, and A. Barthelemy, "Measurement of phase shifts introduced by nonlinear optical phenomena on subpicosecond pulses," *Opt. Lett.*, vol. 14, pp. 275–277, 1989.
[38] D. Strickland and P. B. Corkum, "Resistance of short pulses to self-focusing," *J. Opt. Soc. Amer. B*, vol. 11, pp. 492–497, 1994.
[39] M. Sheik-Bahae, A. A. Said, T.-H. Wei, D. J. Hagan, and E. W. Van Stryland, "Sensitive measurement of optical nonlinearities using a single beam," *IEEE J. Quantum Electron.*, vol. 26, pp. 760–769, 1990.
[40] T. D. Krauss and F. W. Wise, "Femtosecond measurement of nonlinear absorption and refraction in solids," *Appl. Phys. Lett.*, vol. 65, pp. 1739–1741, 1994.
[41] C. Yan and J.-C. Diels, "Amplitude and phase recording of ultrashort pulses," *J. Opt. Soc. Amer. B*, vol. 8, pp. 1259–1263, 1991.
[42] J. L. A. Chilla and O. E. Martinez, "Direct determination of the amplitude and the phase of femtosecond light pulses," *Opt. Lett.*, vol. 16, pp. 39–41, 1991.
[43] D. J. Kane and R. Trebino, "Single-shot measurement of the intensity and phase of an arbitrary ultrashort pulse by using frequency-resolved optical gating," *Opt. Lett.*, vol. 18, pp. 823–825, 1993.
[44] B. S. Prade, J. M. Schins, E. T. J. Nibbering, M. A. Franco, and A. Mysyrowicz, "A simple method for the determination of the intensity and phase of ultrashort optical pulses," *Opt. Commun.*, vol. 113, pp. 79–94, 1994.
[45] J.-K. Rhee, T. S. Sosnowski, A.-C. Tien, and T. B. Norris, "Real-time dispersion analyzer of femtosecond laser pulses with use of a spectrally and temporally resolved upconversion technique," *J. Opt. Soc. Amer. B*, vol. 13, pp. 1780–1785, 1996.
[46] S. Prein, S. Diddams, and J.-C. Diels, "Complete characterization of femtosecond pulses using an all-electronic detector," *Opt. Commun.*, vol. 123, pp. 567–573, 1996.
[47] C. Iaconis and I. A. Walmsley, "Spectral phase interferometry for direct electric-field reconstruction of ultrashort optical pulses," *Opt. Lett.*, vol. 23, pp. 792–794, 1998.
[48] H. R. Lange, M. A. Franco, J.-F. Ripoche, B. S. Prade, P. Rousseau, and A. Mysyrowicz, "Reconstruction of the time profile of femtosecond laser pulses through cross-phase modulation," *IEEE J. Select. Topics Quantum Electron.*, vol. 4, pp. 295–300, 1998.
[49] R. Trebino, K. W. DeLong, D. N. Fittinghoff, J. N. Sweetser, M. A. Krumbügel, B. A. Richman, and D. J. Kane, "Measuring ultrashort laser pulses in the time-frequency domain using frequency-resolved optical gating," *Rev. Sci. Instrum.*, vol. 68, pp. 3277–3295, 1997.
[50] G. Taft, A. Rundquist, M. M. Murnane, H. C. Kapteyn, K. W. DeLong, R. Trebino, and I. P. Christov, "Ultrashort optical waveform measurements using frequency-resolved optical gating," *Opt. Lett.*, vol. 20, pp. 743–745, 1995.
[51] G. Taft, A. Rundquist, M. M. Murnane, I. P. Christov, H. C. Kapteyn, K. W. DeLong, D. N. Fittinghoff, M. A. Krumbügel, J. N. Sweetser, and R. Trebino, "Measurement of 10-fs laser pulses," *IEEE J. Select. Topics Quantum Electron.*, vol. 2, pp. 575–585, 1996.
[52] A. Baltuska, M. S. Pshenichnikov, and D. A. Wiersma, "Amplitude and phase characterization of 4.5-fs pulses by frequency-resolved optical gating," *Opt. Lett.*, vol. 23, pp. 1474–1476, 1998.
[53] A. J. Taylor, G. Rodriguez, and T. S. Clement, "Determination of n_2 by direct measurement of the optical phase," *Opt. Lett.*, vol. 21, pp. 1812–1814, 1996.
[54] J. M. Dudley, L. P. Barry, P. G. Bollond, J. D. Harvey, R. Leonhardt, and P. D. Drummond, "Direct measurement of pulse distortion near the zero-dispersion wavelength in an optical fiber by frequency-resolved optical gating," *Opt. Lett.*, vol. 22, pp. 457–459, 1997.
[55] C. W. Siders, A. J. Taylor, and M. C. Downer, "Multipulse interferometric frequency-resolved optical gating: Real-time phase-sensitive imaging of ultrafast dynamics," *Opt. Lett.*, vol. 22, pp. 624–626, 1997.
[56] E. T. J. Nibbering, O. Dühr, and G. Korn, "Generation of intense tunable 20-fs pulses near 400 nm by use of a gas-filled hollow waveguide," *Opt. Lett.*, vol. 22, pp. 1335–1337, 1997.
[57] C. G. Durfee, III, S. Backus, H. C. Kapteyn, and M. M. Murnane, "Amplitude and phase characterization of 10 fs pulses generated by hollow-core fiber pulse compression," in *Applications of High Field and Short Wavelength Sources VII, Vol. 7, 1997 OSA Tech. Dig. Ser.*, pp. 251–253.
[58] S. A. Diddams, H. K. Eaton, A. A. Zozulya, and T. S. Clement, "Amplitude and phase measurements of femtosecond pulse splitting in nonlinear dispersive media," *Opt. Lett.*, vol. 23, pp. 379–381, 1998.
[59] S. A. Diddams, H. K. Eaton, A. A. Zozulya, and T. S. Clement, "Characterizing the nonlinear propagation of femtosecond pulses in bulk media," *IEEE J. Select. Topics Quantum Electron.*, vol. 4, pp. 306–316, 1998.
[60] R. W. Boyd, *Nonlinear Optics*. San Diego, CA: Academic, 1992.
[61] A. M. Weiner, "Effect of group velocity mismatch on the measurement of ultrashort optical pulses via second harmonic generation," *IEEE J. Quantum Electron.*, vol. QE-19, pp. 1276–1283, 1983.
[62] A. A. Zozulya, S. A. Diddams, A. G. VanEngen, and T. S. Clement, "Propagation dynamics of intense femtosecond pulses: Multiple splittings, coalescence and continuum generation," *Phys. Rev. Lett.*, vol. 82, no. 7, pp. 1430–1433, 1999.
[63] A. G. Van Engen, JILA, University of Colorado, private communication.
[64] E. T. J. Nibbering, M. A. Franco, B. S. Prade, G. Grillon, C. LeBlanc, and A. Mysyrowicz, "Measurement of the nonlinear refractive index of transparent materials by spectral analysis after nonlinear propagation," *Opt. Commun.*, vol. 119, pp. 479, 1995.
[65] P. P. Ho and R. R. Alfano, "Optical Kerr effect in liquids," *Phys. Rev. A*, vol. 20, pp. 2170–2187, 1979.

Hilary K. Eaton received the B.S. degree in chemistry from Furman University, Greenville, SC in 1993. She is currently working toward the Ph.D. degree in physical chemistry at the University of Colorado, Boulder.

Tracy S. Clement (S'89–M'92) received the Ph.D. degree in electrical engineering from Rice University, Austin, TX, in 1993. Her Ph.D. research involved developing and studying short wavelength (XUV and VUV) lasers and ultrashort pulse laser systems.

She is currently a Research Scientist with the optoelectronic devision of the National Institute of Standards and Technology, Boulder, CO. From 1995 to 1998, she was at JILA, University of Boulder, Boulder, CO, where she was a Staff Physicist with the National Institute of Standards and Technology and an Assistant Professor Adjoint in the Department of Physics at the University of Colorado, Boulder. From 1993 to 1995, she was a Director's Postdoctoral Fellow at Los Alamos National Laboratory, Los Alamos, NM. Her current research interests are in ultrafast laser systems, nonlinear optics, and high-intensity light–material interactions.

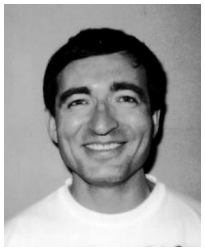

Alex A. Zozulya received the B.Sc. degree in physics from Moscow Engineering Physical Institute in 1978 and the Ph.D. degree in theoretical and mathematical physics from Lebedev Physics Institute of the Academy of Sciences of the U.S.S.R. in 1984.

He is presently with the Department of Physics, Worcester Polytechnic Institute, Worcester, MA. His main research interests include plasma physics, photorefractive nonlinear optics, spatio-temporal solitons, propagation of ultrashort pulses, and atom optics.

Scott A. Diddams received the B.A. degree in physics from Bethel College, St. Paul, MN, in 1989 and the Ph.D. degree in optical science from the University of New Mexico, Albuquerque, in 1996.

While at the University of New Mexico, he was a graduate fellow of the Center for Advanced Studies of the Department of Physics and Astronomy. Currently, he is a National Research Council/National Institute of Standards and Technology Post-Doctoral Fellow at JILA, University of Colorado, Boulder. His research interests include ultrafast optics and phenomena, atomic spectroscopy, and precision measurements.